Electric-field-dictated phase diagram and accelerated dynamics of a reentrant nematic liquid crystal under photostimulation

S Sridevi, S. Krishna Prasad,* and Geetha G. Nair
Centre for Liquid Crystal Research, Jalahalli, Bangalore 560 013, India
(Received 24 June 2009; published 28 August 2009)

In a system consisting of photoactive molecules that exhibit light-driven isomerization transformations, actinic light can diminish or enhance ordering to the extent that transitions from the equilibrium to a more disordered phase can be brought about isothermally. This feature enables light to be used as a thermodynamiclike parameter to investigate phase behavior and adds another dimension to the studies owing to the nonequilibrium character of the isothermal transitions. We have carried out experiments which exploit the combination of two recent findings, viz., an electric field can accelerate the return to the nematic liquid crystalline phase from a photodriven isotropic phase; and in a reentrant mesogen, the photoinduced phase can be more ordered. To photostimulate the nonequilibrium transitions a low power uv radiation (0.1 mW cm^{-2}) has been used. Unique temperature–electric-field phase diagrams of a liquid crystal exhibiting isotropic–nematic–smectic-*A* –reentrant nematic sequence, mapped using light transmission as probe reveal that the electric field influences all the transitions, but the effect is maximum on the equilibrium reentrant nematic to the photoinduced smectic-*A* transition. Temporal measurements have been performed under nonequilibrium conditions to study the dynamics of both the photochemical and the back relaxation processes across the different transitions. The electric field is indeed observed to accelerate the thermal back relaxation in each case, and especially the recovery of the reentrant phase is hastened by three orders of magnitude in time. We explore possible causes for the acceleration and present a finding which can be associated with one of the predictions of density-functional calculations for isomerization of azobenzenes.

DOI: 10.1103/PhysRevE.80.021703 PACS number(s): 42.70.Gi, 68.35.Rh, 64.70.M−, 64.75.Yz

I. INTRODUCTION

A system is said to undergo a "reentrant" phase transition, if a monotonic variation in any thermodynamic field such as temperature or pressure results in two (or sometimes more) phase changes and finally attains a state which is macroscopically similar to the initial state. This phenomenon is exhibited by amazingly diverse condensed-matter systems [1–5]. In liquid crystals (LCs) such a phenomenon was discovered with the observation of a nematic–smectic-*A* (Sm-*A*)–reentrant nematic sequence, in the temperature-concentration [6] and temperature-pressure planes [7]. LC systems especially have proved to be very rich in exhibiting the phenomenon of reentrance involving a diverse number of phase transitions, namely, nematic–smectic-*A* (including double [8] and triple [9] reentrant sequences), ferroelectric-ferrielectric, ferrielectric-antiferroelectric smectics [10], twist grain boundary–smectic-*A* [11], synclinic-anticlinic [12], uniaxial-biaxial nematic [13], and uniaxial–biaxial smectic-*A* [14] transformations. Recently [15], we have demonstrated that a third albeit nonthermodynamic parameter, viz., actinic light can be employed to induce the reentrant nematic sequence in a system that does not exhibit it in the normal thermal process. The principle behind this light-induced phase transition is the phenomenon of reversible photoinduced shape transformation of chromophoric molecules, such as azobenzenes, a topic that has been extensively studied [16]. The azobenzene molecule has been particularly attractive for photoinduced phase transitions, to be discussed below, due to its easily accomplished geometric isomerization about the azo bond, converting the molecule from *E* to *Z* isomer. For this reason it has been employed for altering molecular, macroscopic, and even biological properties [17]. Upon uv irradiation (wavelength of ~360 nm, corresponding to the π-π^* band of the azo group), the energetically more stable *E* configuration with an elongated rodlike molecular form changes into the bent *Z* configuration. The reverse transformation can be brought about by illuminating with visible light (~450 nm, corresponding to the n-π^* band). This latter change can also occur spontaneously in the "dark" by a process known as *thermal back relaxation* (TBR). The liquid crystalline phase is stabilized by the rodlike *E* form, but is destabilized by the bent *Z* form. Therefore, the *E*-*Z* change generally leads to a diminution of the transition temperature, which—if substantial—causes an isothermal photoinduced transition from a liquid crystalline phase, say, the nematic phase to the isotropic phase. Such light-driven transitions have been observed for a variety of systems exhibiting different phases [18]. A general feature of such transformations is that the photoinduced phase would be more disordered than the equilibrium one. We reported an exception to such an established principle in a system where the photoisomerization drives the system to the layered Sm-*A* phase from the disordered reentrant nematic present under equilibrium conditions [15,19].

The time taken for the phase transition to take place following the isomerization of the photoactive molecules is of significant interest not only from a basic point of view, but it also has paramount significance especially for applications such as storage devices [20]. For the photoinduced nematic-isotropic (*N*-*I*) transition the time τ_{ON} required for the

*skpras@gmail.com

change (following the *E-Z* isomerization) to occur, the typical duration required is on the order of a few minutes with a conventional type of uv source, but very fast time scales can be achieved with a pulsed laser source [19]. In contrast, τ_{off}, the thermal back relaxation time restoring the *N* phase, takes much longer (at least an order of magnitude more). In fact, it is this longer τ_{off} that puts a limitation on the time response of dynamic optical devices. Although illuminating the sample with longer wavelength (around 420 nm) light hastens the reverse isomerization, the process however increases the complexity of the system by the requirement of a second light source and the associated problems of having the aligning optics. In this context the recent development [21] that an applied electric field can accelerate the relaxation to the equilibrium from the photodriven state is important. We found that the acceleration is as fast as that could be achieved by the longer wavelength light and the actual response time can be fine tuned by controlling the magnitude of the electric field. In contrast to equilibrium cases, nonequilibrium phase transitions are yet to be understood, owing to the sheer diversity of systems which exhibit such transformations involving physical, chemical, biological, and even sociological situations [22]. In the photoinduced transitions mentioned above, the isomerization and the resulting phase change drive the system away from equilibrium conditions and thus provide a convenient situation to study nonequilibrium transitions, and also an additional motivation for the present work.

In this paper we map out unique temperature–electric-field phase diagrams obtained under nonequilibrium conditions. We also demonstrate that electric-field-assisted acceleration of the back relaxation process is general and applicable to layered as well as the reentrant systems. More specifically, we show that the magnitude of the acceleration for a given voltage is dependent on the nature of the equilibrium and photoinduced phases also. We discuss possible mechanisms for this acceleration by considering among other things the quantum chemical calculations reported earlier [23].

II. EXPERIMENT

The host liquid crystalline material was the binary mixture of the eighth (C_8) and the tenth (C_{10}) homologs of the series 4-(2-cyanoethyl) phenyl-4-(alkoxy) benzoate in 30:70 ratio by weight. While C_{10} exhibits the isotropic (iso)–Sm-*A*–smectic-*C* (Sm-*C*) sequence, C_8 shows only the iso-nematic (*N*) transition [24]. The uv active dopant 4-(4-ethoxy phenylazo) phenyl hexanoate (EPH) (Kodak Organics), also liquid crystalline, acts as the guest compound and is added at a concentration of 3% (by weight) to the host material.

Details of the pump-probe beam setup used for the static and dynamic measurements both in the presence and in the absence of uv light are described elsewhere [15]. Briefly, the probe beam (He-Ne laser) intensity transmitted through the sample was collected using a photodetector and measured using a digital multimeter. The photoisomerization was brought about by employing uv radiation from an intensity stabilized uv source (Hamamatsu) equipped with a fiber-optic guide and a narrow bandwidth uv-pass visible cut filter used to select the desired radiation of ~365 nm. A programmable temperature controlled hot stage (Mettler FP82) was used to control the sample temperature. The liquid crystal cell consisted of a pair of indium tin oxide (ITO)-coated glass plates with a cell gap in the range of 10–12 μm. The inner surface of one of the glass plate was coated with polyimide to get planar alignment and that of the other with silane solution to promote homeotropic alignment of liquid crystalline molecules. The cell fabricated using these two glass plates resulted in a *hybrid* geometry.

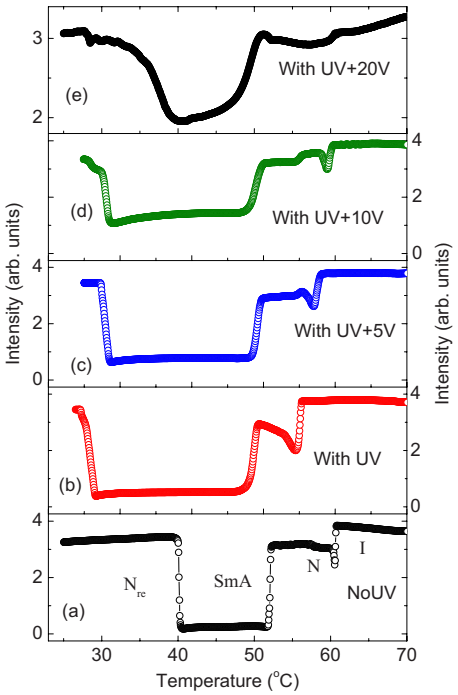

FIG. 1. (Color online) Scans of the laser transmitted intensity as a function of temperature (a) in the absence of and (b) upon shining uv light (0.1 mW cm^{-2}). Panels (c), (d), and (e) show the effect of different magnitudes of voltage when the uv light is simultaneously present.

III. RESULTS AND DISCUSSION

A. Static measurements and phase diagram

Figure 1 shows the raw intensity scans obtained for the pristine sample, and while being illuminated with a low magnitude uv intensity of $I_{uv}=100$ μW/cm^2 in situations where an applied electric field is absent or present. The first feature to note is that all the three transitions, *I-N*, *N*–Sm-*A*, and Sm-*A*-N_{re}, exhibit a lowering of the transition temperature upon photoisomerization driven by the uv illumination. However, the magnitude of this shift in the transition temperature ΔT is least for the *N*–Sm-*A* transition, intermediate for *I-N*, and maximum for the Sm-*A*-N_{re} transformation. Such an enhanced destabilization of the N_{re} phase has been observed by us earlier [19] and argued to be due to a combination of the photodriven nanophase segregation [25] and

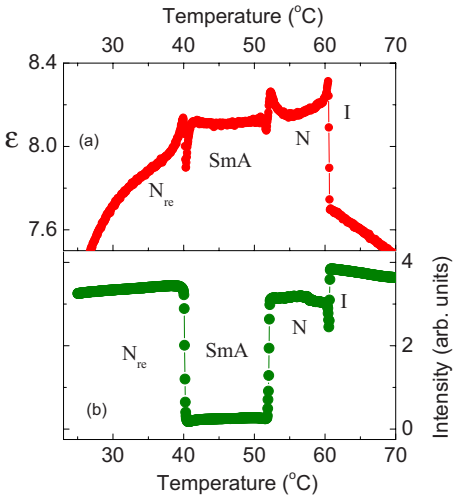

FIG. 2. (Color online) Diagram to show that clear signatures of the transitions are observed in the (a) capacitance as well as (b) transmitted light intensity measurements also.

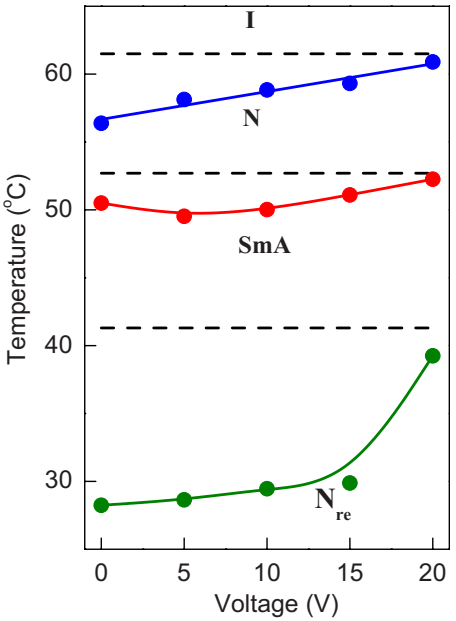

FIG. 3. (Color online) Temperature-voltage phase diagram. The dashed lines represent the transition temperatures obtained in the absence of photostimulation. The filled circles are the transition temperatures obtained when the sample is illuminated with uv radiation. The lines through the data points are only guides to the eye. Notice that the electric field drastically affects the Sm-A-N_{re} transition and that with about 20 V the photoinduced diminution in the transition temperature is nearly annulled.

the frustrated spin-gas situation [26]. Recently [21], we discovered that the magnitude of ΔT for the I-N transition is altered if an electric field is applied. This study also found that the effect is the strongest for dc field and diminishes for ac field of increasing frequency. Therefore, the present measurements were performed employing only dc voltages. The scans presented in the upper three panels of Fig. 1 were obtained by applying the mentioned voltages while simultaneously illuminating the sample with uv radiation. Not only I-N, but the other two transitions also show that application of the electric field reduces the *diminution in the transition temperature effect* imparted by the uv radiation through photoisomerization. A point that must be mentioned is that the employed material has a positive dielectric anisotropy, i.e., $\Delta\varepsilon=\varepsilon_{\parallel}-\varepsilon_{\perp}>0$, where $\varepsilon_{\parallel}$ and $\varepsilon_{\perp}$ represent the dielectric constants parallel and perpendicular to the director direction, respectively. For such a material the nematic director couples to the electric field and if the voltage is large enough gets oriented along the field direction. The hybrid geometry of the sample cell makes the molecules parallel to the substrate at one surface and perpendicular to it at the other. Therefore, at least in the two nematic phases, the configuration would be that of a uniform bend deformation in the absence (and also for low values) of the electric field. Such a geometry is known to yield large changes in the transmitted light intensity across the N (or N_{re})–Sm-A transition. When the field is large enough a large majority of the molecules would be aligned along the field direction resulting in a near-uniform homeotropic alignment. In such a case, the change across the transition would be much smaller, which explains a smaller variation in intensity for the 20 V case shown in Fig. 1. In fact, the transitions can be clearly followed with dielectric constant measurements as well, as shown in Fig. 2, and confirm the identification of the transformations made using the light transmission data. However, the signatures become much weaker for high voltages for the reason mentioned above and therefore in the rest of the paper we describe intensity changes for keeping track of the transitions.

Figure 3 shows the temperature–electric-field phase diagram realized from measurements without and with uv illumination. The large influence of photoisomerization on the N_{re}-Sm-A transition and the varied influences of the electric field on the different transitions are clearly seen. The interesting features are that (i) when the voltage is 20 V (field of ~ 2 V/μm) the photodriven reduction in the transition temperatures is nearly annulled; (ii) the rate at which such an annulment takes place is not the same for the different transitions; and (iii) whereas the phase lines obtained without uv (dashed lines in Fig. 3) represent equilibrium transitions, the boundaries realized with uv illumination (with or without voltage, solid lines through the data sets) are nonequilibrium situations. This is due to the fact that the Z isomers responsible for such a feature revert eventually to the E form spontaneously. Therefore, the actual coordinates of the "with uv" phase lines are dependent on various extrinsic parameters such as the amplitude of the uv intensity, the E-Z conversion efficiency of the photoactive guest molecule, etc. We shall return to these points later.

B. Dynamics

1. ON process

As mentioned in the Introduction, the photochemical transition (triggered by the equilibrium E to the photodriven Z conformer), also referred to as the ON process here, is fast, occurring on the time scale of minutes in the case of the N-I transformation. The temporal variations in the transmitted intensity when the photodriven N-I, Sm-A-N, and N_{re}–Sm-A transitions take place from the equilibrium N, Sm-A, and N_{re}

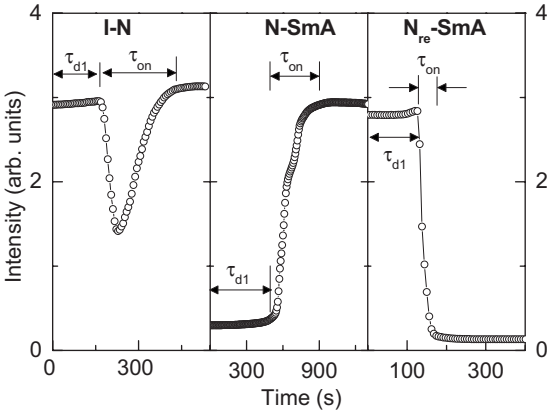

FIG. 4. The time-resolved variation in the transmitted intensity when the uv light is turned on at time=0 instant, keeping the sample temperature 2 °C below the respective equilibrium transition temperature. The notations used to define the delay (τ_{d1}) and the response (τ_{on}) times are shown. Particularly, notice that the N_{re}-Sm-*A* transition has the sharpest response.

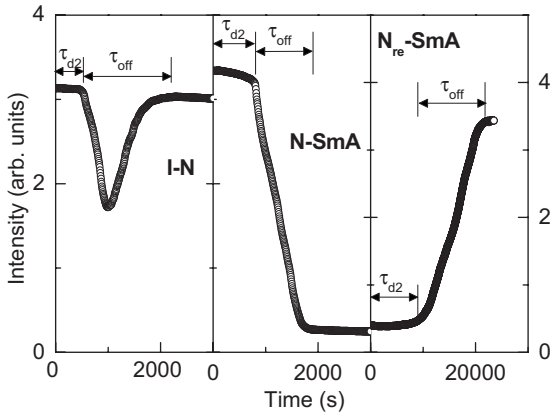

FIG. 5. The time-resolved variation in the transmitted intensity after the uv illumination is turned off, while the sample temperature is maintained 2 °C below the respective equilibrium transition temperature. The notations used to define the delay (τ_{d2}) and the response (τ_{off}) times are shown. Particularly, notice that the thermal back relaxation process for the recovery of the N_{re} phase (Sm-*A*-N_{re} transition) takes much longer than in the case of the other two phases.

phases, respectively, are shown in Fig. 4 (during these measurements the sample temperature was maintained 2 °C below the respective equilibrium transitions). The signatures of these isothermal transitions are quite similar to their thermodynamics counterparts shown in Fig. 1. Notice that, for all the temporal transitions, the sample response starts only after a delay from the instant at which the uv radiation is switched on. We quantify this in terms of a delay time τ_{d1}. It is interesting to note that τ_{d1} values are not very different for the *N*-*I* and Sm-*A*-*N* transitions; it is substantially (~factor of 3; see Table I) faster for the case where *E*-*Z* isomerization enhances the order in the medium, viz., the N_{re}–Sm-*A* transition. The actual response itself, quantified by τ_{on}, is also faster for the N_{re}–Sm-*A* transition, a feature that we had noticed in an earlier experiment also [19]. A possible cause for this faster disappearance of the N_{re} phase to the Sm-*A* phase could be the photodriven nanophase segregation, a feature which will be explained in the next section. A second possibility is the fact that the N_{re}–Sm-*A* transition is most sensitive to photoisomerization related effects as can, for example, be seen in the magnitude of the photodriven shift in the transition temperature; very large magnitudes of the shift can be obtained with extremely low levels of uv intensity, a feature indeed seen in our previous work. This can be interpreted to mean that even a small perturbation is enough to drive the N_{re} phase to a layered structure, thus achieving a faster dynamics. This argument is in fact supported by the thermal back relaxation behavior of the system, to be discussed below.

TABLE I. The delay and response times for the photostimulated change across the different transitions.

Transition	τ_{d1} (s)	τ_{ON} (s)
N-*I*	163	431
Sm-*A*-*N*	490	899
N_{re}–Sm-*A*	128	194

2. Thermal back relaxation (off) process

The TBR is generally a slow process, especially with azobenzenes as the photoactive molecules. The kinetics of this relaxation to the equilibrium phase from the photodriven was also monitored using temporal measurements of the transmitted intensity. Figure 5 displays the TBR process from the photodriven *I*, *N*, and Sm-*A* to the equilibrium *N*, Sm-*A*, and N_{re} phases, respectively. Here again the data exhibits a delay time τ_{d2} and a response time τ_{off}. The delay increases in a monotonic fashion with lowering of the temperature, being shortest for the *I*-*N* transition and longest for the Sm-*A*-N_{re} transition. But this is not true for the response time τ_{off}. However, the point to be noted is that whereas the durations have comparable values for the *I*-*N* and *N*–Sm-*A* transitions, the recovery of the N_{re} phase occurs with nearly an order of magnitude longer delay as well as response times. Indeed, this last feature has been observed earlier [19]. A simple inspection of the data (especially the nonmonotonicity of the response times) indicates that the longer duration for the recovery of the N_{re} phase cannot be explained as merely due to a thermally activated process governed by an exponential variation. In fact, in an earlier work we had proposed [19] that the photocontrolled nanophase segregation mechanism postulated by the Boulder group [25] in conjunction with the frustrated spin-gas model of the MIT group [26] can explain such an observation. We shall recall this argument briefly here.

First, it may be recalled that the very appearance of the Sm-*A* phase in any liquid crystalline phase is expected to be because of a well-developed segregation of the aromatic and aliphatic parts of the molecule, while in the normal cases the segregation is established at the time of the synthesis itself owing to the chemical structure of the molecule. In contrast, the photocontrolled nanophase segregation is an on-demand separation produced when the guest photoactive part of a (guest-host) system is isomerized. The principle behind this

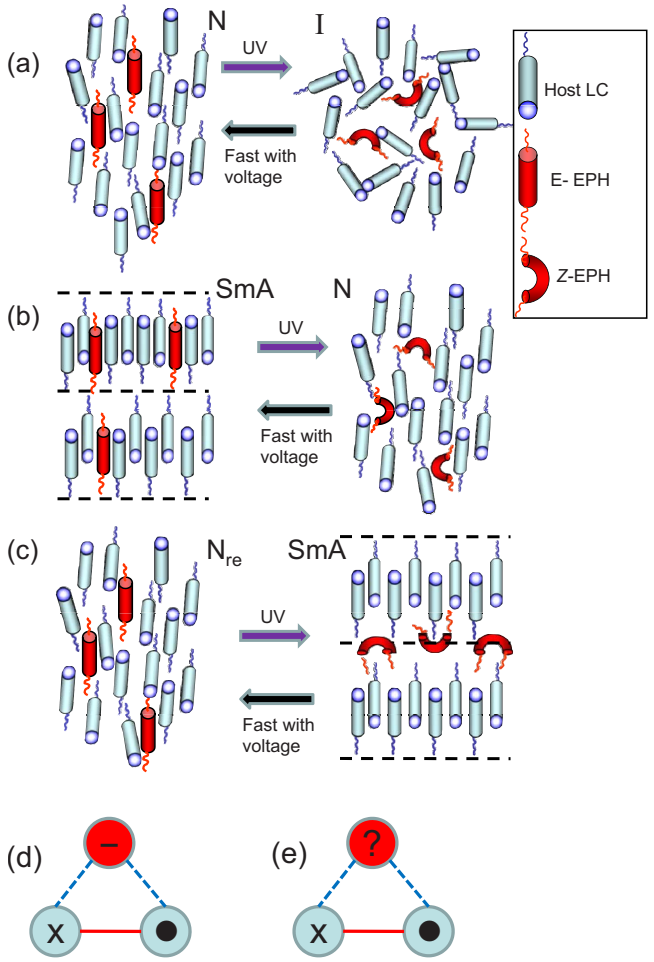

FIG. 6. (Color online) (a)–(c) Schematic representation of the molecular arrangements in the equilibrium (left panels) and photodriven (right panels) states. Notice especially the nanophase segregation in the photostimulated Sm-*A* phase (panel c). (d) and (e) Configuration of triplet of molecules, with the cyan (gray) colored circles representing host polar LC molecules and the red (dark) colored circles representing the photoactive EPH molecules. The dot and the cross in the center indicate dipoles pointing into or out of the plane. The red (solid) and the blue (dashed) lines indicate the interactions. In (d) the EPH molecule is in its *E* state with negligible dipole moment and therefore does not cause a frustration in the triplet, whereas in the *Z* form it does [indicated by the question mark in (e)] due to the large value of the dipole moment.

nanophase segregation (see Fig. 6) is that when the uv radiation is absent the azo molecules are in their *rodlike E* form and are thus easily accommodated into the smectic layers. But the bent form of its photoinduced *Z* form is disliked by the rodlike host molecules and is consequently expelled from within to a region between the host layers.

The frustrated spin-gas model, found to describe the reentrant transitions quite well, is essentially designed for molecules having a strong terminal polar group like the ones in the host mixture used here. In the Sm-*A* phase of such systems, the aim to minimize frustration arising due to possible ferroelectric and antiferroelectric interactions of the neighboring molecules generates notches in the free-energy minimum. If the situation favors the molecules to permeate or diffuse from one smectic layer to the next one, the layer gets destabilized and, consequently, the nematic phase reenters. On the other hand, if the presence of the triplet dipoles is favored, the smectic order is stabilized through short-range dipolar interactions. In the nanophase segregated case, although thermally the N_{re} phase is the favored one, the disliking between the bent photoactive molecules (in their *Z* form) and the host rodlike molecules stabilizes the Sm-*A* phase better. This first manifests as an extended range for the smectic phase when the light is shined (see Figs. 1 and 3). Second, in the dynamic sense it makes the escape from the N_{re} phase faster (faster τ_{on} for the N_{re}–Sm-*A* phase) and retards the recovery of the N_{re} phase (slower TBR). This tendency to avoid the N_{re} phase is so strong that substantial effects are seen even for very low powers of the uv intensity. The question that may arise at this point is that if the above arguments are true then why such effects are not observed (at least not as strongly) for the high-temperature Sm-*A*-*N* transition. We believe that the opposition from the larger thermal fluctuations (higher temperature), favoring disorder in the medium reduces the effect. However, the nanophase segregation may still dominate given a chance and perhaps is the cause for the faster τ_{off} seen for the *N*-Sm-*A* transition, in comparison to that for the *I*-*N* transition. As far as the dynamics is concerned, the point to be noticed in Fig. 6(a) is that, in the case of the relaxation of *N* from the photodriven *I* phase, the host molecules need to simply change their orientation. In the Sm-*A*-*N* case, the back relaxation from the fluid *N* phase to the one-dimensionally ordered state of Sm-*A* may be relatively easier, since the bent photoactive molecules are present in a fluid environment [Fig. 6(b)]. In contrast, the nanophase segregated Sm-*A* phase photodriven from the fluid N_{re} phase has the bent azo molecules trapped in the one-dimensional periodic potential of the layered structure [Fig. 6(c)]. Therefore, the recovery of the N_{re} phase can be visualized to be more complicated, involving first the transformation of the *Z* conformers to the *E* form and then sliding down to random positions along the director direction to get rid of the layering. This is what we believe to be the reason for the longer duration of TBR.

It must be recalled that the presence of the azobenzene molecules, having weak polarity in the *E* configuration alters the process of interaction between the molecules. The triplet-molecule-induced frustration mentioned above could be reduced [Fig. 6(d)] if one of the molecules in the triplet is a nonpolar one (the effect is not large owing to the low concentration of the photoactive molecules used here). A further parameter that should be considered is the charge transfer complex that can get formed [27] between strongly polar host molecules which act as acceptors and the weakly polar photoactive molecules as donors. However, what perhaps plays the major role is the enhanced dipole moment of the *Z* isomer ($\sim 5D$) coupled with its packing constraint owing to the bent shape. At least in the situation when segregation occurs, the bent *Z* conformers would want to pack such that their bend direction is along the layer normal and therefore effectively interacting with the host polar molecules aiding the frustration [Fig. 6(e)] and consequent phase sequences in the medium. This may be the cause for the enhancement of the smectic range upon photoisomerization. A caveat that

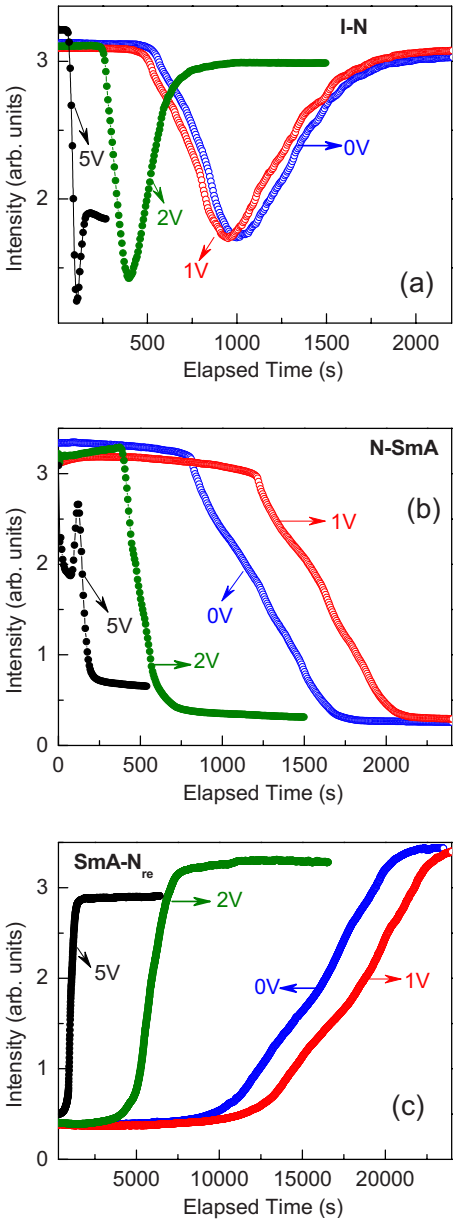

FIG. 7. (Color online) Temporal behavior of the transmitted intensity as a function of the time elapsed since the uv is turned off and simultaneously the voltage of different magnitudes is turned on during the thermally back relaxation of the (a) *I*-*N*, (b) *N*–Sm-*A*, and (c) Sm-*A*-N_{re} transitions. Notice that generally with increasing voltage the process is hastened, with the effect being large for the Sm-*A*-N_{re} transition. However, the 1 V data for the latter two transitions deviate from this behavior.

must be added is that, due to the low concentration of the photoactive molecules, these effects would be perturbative in nature.

3. Electric field effect

The temporal variations in the transmitted intensity during the back relaxation process of the three transitions, upon application of voltage of different magnitudes, are shown in Fig. 7. A common feature seen for all the three transitions is

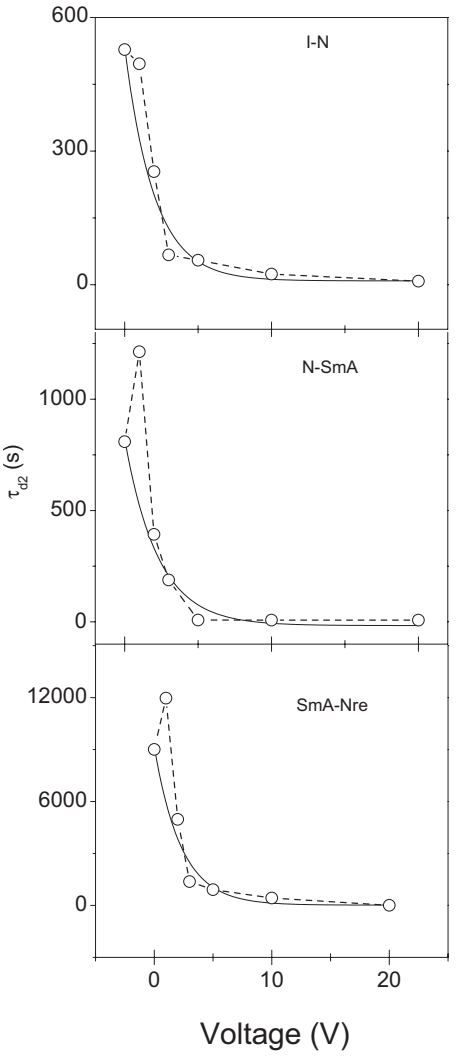

FIG. 8. Dependence of the delay time τ_{d2}, for the thermal back relaxation process on the applied voltage for the *I*-*N*, *N*–Sm-*A*, and Sm-*A*-N_{re} transitions. The dashed lines merely connect the data points to illustrate the nonmonotonic behavior around 1 V. The solid lines are fits obtained to an exponential decay function performed by excluding the data for 1 V.

that the presence of the electric field generally accelerates the recovery of the equilibrium situation and appears to have a limiting behavior at larger voltages. A second feature to be noted is that the profiles become sharper and change their appearance also with voltage. The former indicates that not only the delay time, but also the response time is affected by the voltage. The latter is due to the fact that the system having a positive dielectric anisotropy and therefore the molecules would want to get reoriented along the field direction at sufficiently high voltages. The third feature is that, unlike for the *I*-*N* transition, the transitions associated with the Sm-*A* phase exhibit, in comparison to the no-voltage thermal back relaxation, longer delay as well as response times when the voltage applied is 1 V. This is clearly seen in the plots of τ_{d2} and τ_{off} as functions of the applied voltage [Figs. 8 and 9]. The influence of the voltage is not only on the duration of the delay, but also on the response time. This is at variance with the behavior observed when a surface field is dominant,

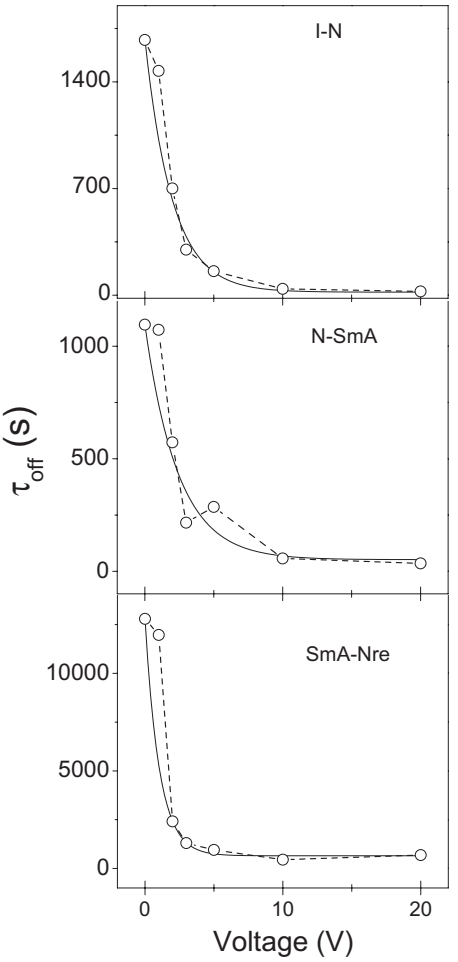

FIG. 9. Dependence of τ_{off}, the response time for the thermal back relaxation process on the applied voltage for the *I*-*N*, *N*–Sm-*A*, and Sm-*A*-N_{re} transitions. The dashed lines merely connect the data points to illustrate the nonmonotonic behavior around 1 V. The solid lines are fits obtained to an exponential decay function performed by excluding the data for 1 V.

a point that will be discussed later. When the voltage is 20 V, τ_{d2} for all the three transitions reduces to about 8 s, a value which is close to the time interval at which the data are collected (6 s). The effect of the electric field in diminishing τ_{d2} is maximum in the case of the *N*–Sm-*A* transition: even at a voltage of 5 V, it achieves this limiting value, as compared to the values of 55 and 909 s for the *I*-*N* and Sm-*A*-N_{re} transitions. However, the largest acceleration in τ_{d2} is seen for the Sm-*A*-N_{re} transition at larger voltages: at least three orders of magnitude. In contrast, the improvement in the response times upon application of voltage is more modest. In the absence of any theoretical model that describes the influence of an applied electric field on TBR, we have fitted the data, by excluding the value obtained for 1 V, to an exponential decay function. As shown by the solid lines in Figs. 8 and 9, this function fits the data reasonably well. The reason for both the features, namely, that the exponential form describes the data and that there is an increase in the value for 1 V are not clear to us.

Now we look at the possible causes for the acceleration of the back relaxation when an electric field is present. First, let us recall that a drastic diminution in the delay time (and not in the response time) has been observed for the recovery of the equilibrium *N* phase from the photoinduced *I* phase, when the material is confined in a polymer matrix, and has been argued to be due to the presence of virtual surfaces at each liquid-crystal–matrix interface [28]. The virtual surfaces create a surface field that is known to enhance the nematic ordering [29]. In the photoinduced isotropic case, the surface field produces a paranematiclike situation and thus reduces the delay time in the return to the equilibrium *N* phase, but does not alter the process once the first nematic droplets appear, and therefore the response time is unaltered. This is the essential difference between such a virtual surface field and the external electric field of the present case, with the latter reducing the delay as well as the response times. Since the virtual surface field appeals to the molecular anchoring at such interfaces, the chemical nature of the host molecules also become important. In the electric field case, we have previously observed [21] that strong as well as weakly polar host molecules get significantly influenced. This provides the first clue that perhaps the dielectric coupling between the host molecules and the electric field may not be a central factor. Also, as reported already, the influence of the electric field is limited to dc and very low frequency electric fields, a behavior not expected if the dielectric coupling were to be the reason. These arguments are further supported by the fact that the other two transitions, *N*–Sm-*A* and Sm-*A*-N_{re}, behave essentially in the same fashion, although the difference in the order parameter across these transitions is not the nematic order parameter. Owing to the fact that the acceleration of the TBR process is seen in the equilibrium isotropic phase also [21] rules out a flexoelectric origin (an effect possible especially because of the bent shaped *Z* isomers). We had previously suggested [21] that the electrode polarization arising in the experimental conditions used is perhaps the underlying cause for the acceleration of the TBR. While this may still be operative in the present case, the different magnitudes of acceleration for the three transitions and also the values being nonmonotonical with temperature indicates that there could be other influences also. An important outcome of these analyses is that perhaps the electric field directly influences the azobenzene molecule itself with the host molecules hardly playing any role. A theoretical model that is under consideration in this regard is density-functional-theory-based calculations by Füchsel *et al.* [23], which proposes that it is possible to induce the isomerization of azobenzene in the gas phase by an electric field; this model has been used to explain electric-field-induced isomerization of an azobenzene derivative on the gold surface by a scanning tunnelling microscope (STM) tip [30]. The theory considers that in the presence of an electric field, the potential-energy surface related to a reaction path can be deformed, thus leading to an effective lowering of the isomerization barrier, and is argued to depend on the orientation of an intrinsic dipole moment (if present) and also on the polarizability of the molecule. The essential point is that application of an electric field reduces the potential barrier between the *E* and *Z* isomers and therefore favors a quicker return of the photoactive molecule to the equilibrium form. Qualitatively this theory can explain the influence of

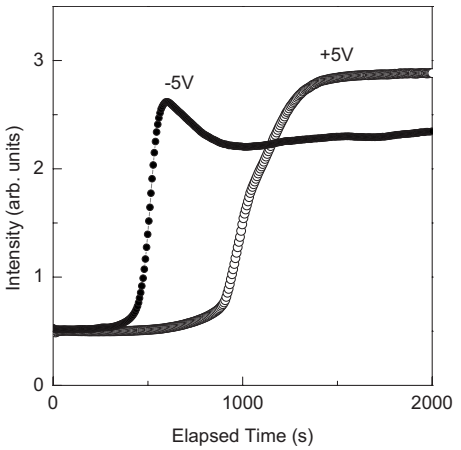

FIG. 10. Temporal dependence of the back relaxation process associated with the recovery of the N_{re} phase from the photostimulated Sm-*A* phase, exhibiting asymmetric behavior for the opposite signs of the applied voltage, with the delay time (τ_{d2}) and response time (τ_{off}) being shorter for the negative voltage.

the electric field on the static as well as dynamic properties that we observe in our experiments. It should however be borne in mind that the actual electric field in our experiments (even at the highest voltage of 20 V) is three orders of magnitude smaller than in the STM experiments.

Finally, we present in Fig. 10 the transmitted intensity during the back relaxation process from the photoinduced Sm-*A* to the N_{re} phase for positive and negative signs of the applied voltage of fixed magnitude (5 V). The sign is defined with respect to the electrode kept closest to the uv source. The asymmetric behavior with the sign of the voltage is obvious. In fact, both the delay and response times are nearly halved for the negative voltage in comparison with the positive voltage. Similar behavior is seen for the *I*-*N* and *N*–Sm-*A* transitions also, with the actual changes in τ_{d2} and τ_{off} being different. These features are interesting since the density-functional theory [23] predicts an asymmetric response in the cis-trans isomerization with the change in the sign of the electric field. These situations correspond to what the authors refer to as model A, in which the intrinsic and induced dipole moments of the *Z* isomer are aligned along the electric field. Here, the orientation of the molecular intrinsic dipole moment with respect to the electric field leads to variation in the voltage required for the isomerization when the sign of the field is changed. The implications of such a comparison need to be investigated.

IV. CONCLUSIONS

We have investigated the influence of electric field on the phase diagram and dynamic properties of photostimulated transitions in a reentrant nematic liquid crystal. The mapped out temperature–electric-field phase diagrams reveal that the electric field influences all the transitions, but its effect is maximum on the equilibrium reentrant nematic to the photoinduced smectic-*A* transformation. The dynamics of both the photochemical and back relaxation processes across the different transitions have been studied under photoinduced nonequilibrium conditions. The electric field accelerates the thermal back relaxation in each case with the recovery of the reentrant phase being about 1000 times faster. Possible causes for the acceleration have been explored and an indication that the acceleration may be associated with the phenomenon predicted by the density-functional theory.

[1] C. S. Hudson, Z. Phys. Chem., Stoechiom. Verwandtschaftsl. **47**, 113 (1904).
[2] G. Ramírez-Santiago and J. V. José, Phys. Rev. B **77**, 064513 (2008); H. W. Meul, C. Rossel, M. Decroux, O. Fischer, G. Remenyi, and A. Briggs, Phys. Rev. Lett. **53**, 497 (1984).
[3] J. Yamanaka, H. Yoshida, T. Koga, N. Ise, and T. Hashimoto, Phys. Rev. Lett. **80**, 5806 (1998); M. J. P. Gingras and E. S. Sorensen, Phys. Rev. B **57**, 10264 (1998).
[4] P. V. Vanitha and C. N. R. Rao, J. Phys.: Condens. Matter **13**, 11707 (2001); S. L. A. de Queiroz, Phys. Rev. B **63**, 214202 (2001).
[5] For a summary of the early work on this phenomenon, see, for a review, T. Narayanan and A. Kumar, Phys. Rep. **249**, 135 (1994).
[6] P. E. Cladis, Phys. Rev. Lett. **35**, 48 (1975).
[7] P. E. Cladis, R. K. Bogardus, W. B. Daniels, and G. N. Taylor, Phys. Rev. Lett. **39**, 720 (1977).
[8] F. Hardouin, G. Sigaud, M. F. Achard, and H. Gasparoux, Phys. Lett. **71A**, 347 (1979).
[9] N. H. Tinh, F. Hardouin, and C. Destrade, J. Phys. (France) **43**, 1127 (1982); R. Shashidhar, B. R. Ratna, V. Surendranath, V. N. Raja, S. Krishna Prasad, and C. Nagabhushan, J. Phys. (France) Lett. **46**, L-445 (1985).
[10] D. S. Shankar Rao, S. Krishna Prasad, S. Chandrasekhar, S. Mery, and R. Shashidhar, Mol. Cryst. Liq. Cryst. **292**, 301 (1997).
[11] D. S. Shankar Rao, S. K. Prasad, V. N. Raja, C. V. Yelamaggad, and S. A. Nagamani, Phys. Rev. Lett. **87**, 085504 (2001); V. Vill and H. W. Tunger, J. Chem. Soc., Chem. Commun. **1995**, 1047.
[12] M. H. Zhu, C. Rosenblatt, J. M. Kim, and M. E. Neubert, Phys. Rev. E **70**, 031702 (2004).
[13] L. J. Yu and A. Saupe, Phys. Rev. Lett. **45**, 1000 (1980).
[14] C. V. Yelamaggad, V. Padmini, D. S. Shankar Rao, Geetha G. Nair, and S. Krishna Prasad, J. Mater. Chem. **19**, 2906 (2009).
[15] S. Krishna Prasad, Geetha G. Nair, and Gurumurthy Hegde, Adv. Mater. **17**, 2086 (2005); J. Phys. Chem. B **111**, 345 (2007).
[16] See, e.g., H. Rau, *Photochemistry and Photophysics* (CRC Press, Boca Raton, FL, 1990), Vol. 2, Chap. 4; R. El Halabieh, O. Mermut, and C. J. Barrett, Pure Appl. Chem. **76**, 1445 (2004).
[17] K. G. Yager and C. J. Barrett, J. Photochem. Photobiol., A **182**, 250 (2006).

[18] For recent reviews on this topic, see S. Krishna Prasad, Geetha G. Nair, Gurumurthy Hegde, K. L. Sandhya, D. S. Shankar Rao, Chethan V. Lobo, and C. V. Yelamaggad, Phase Transitions **78**, 443 (2005); T. Ikeda, J. Mater. Chem. **13**, 2037 (2003); S. Krishna Prasad, Geetha G. Nair, and D. S. Shankar Rao, Liq. Cryst. **36**, 705 (2009).

[19] S. Krishna Prasad and Geetha G. Nair, Adv. Mater. **13**, 40 (2001).

[20] D. Attianese, M. Petrosino, P. Vacca, S. Concilio, P. Iannelli, A. Rubino, and S. Bellone, IEEE Electron Device Lett. **29**, 44 (2008); S. L. Lim, Na-Jun Li, Jian-Mei Lu, Qi-Dan Ling, C. X. Zhu, En-Tang Kang, and K. G. Neoh, ACS Appl. Mater. Interfaces **1**, 60 (2009).

[21] S. Krishna Prasad, Geetha G. Nair, and V. Jayalakshmi, Adv. Mater. **20**, 1363 (2008).

[22] Q. M. Nie, W. Zhou, and Q. H. Chen, Eur. Phys. J. B **65**, 485 (2008); H. E. Stanley, Nature (London) **404**, 718 (2000); D. Walgraef, G. Dewel, and P. Borckmans, Adv. Chem. Phys. **49**, 311 (1982); J. Candia, J. Stat. Mech.: Theory Exp. **2007**, P09001 (2007).

[23] G. Füchsel, T. Klamroth, J. Dokić, and P. Saalfrank, J. Phys. Chem. B **110**, 16337 (2006).

[24] G. Pelzl and D. Demus, Z. Chem. **21**, 151 (1981).

[25] Y. Lansac, M. A. Glaser, N. A. Clark, and O. D. Lavrentovich, Nature (London) **398**, 54 (1999).

[26] A. N. Berker and J. S. Walker, Phys. Rev. Lett. **47**, 1469 (1981).

[27] J. W. Park, C. S. Bak, and M. M. Labes, J. Am. Chem. Soc. **97**, 4398 (1975).

[28] K. L. Sandhya, S. Krishna Prasad, and Geetha G. Nair, Appl. Phys. Lett. **83**, 2707 (2003).

[29] See, e.g., P. A. Kossyrev, J. Qi, N. V. Priezjev, R. A. Pelcovits, and G. P. Crawford, Appl. Phys. Lett. **81**, 2986 (2002).

[30] M. Alemani, Ph.D. dissertation, Free University Berlin, 2006; M. Alemani, F. Moresco, M. V. Peters, S. Hecht, K.-H. Rieder, and L. Grill, J. Am. Chem. Soc. **128**, 14446 (2006).